Exoplanet Imaging with LOCI Processing: Photometry and Astrometry with the New SOSIE Pipeline.

Christian Marois[a], Bruce Macintosh[b] and Jean-Pierre Véran[a]

[a] National Research Council Canada, Herzberg Institute of Astrophysics, 5071 West Saanich Road, Victoria, BC, V9E 2E7, Canada;

[b] Lawrence Livermore National Laboratory, 7000 East Ave., Livermore, California, 94550, USA

ABSTRACT

The Angular, Simultaneous Spectral and Reference Star Differential Imaging techniques (ADI, SSDI and RSDI) are currently the main observing approaches that are being used to pursue large-scale direct exoplanet imaging surveys and will be a key component of next-generation high-contrast imaging instrument science. To allow detection of faint planets, images from these observing techniques are combined in a way to retain the planet flux while subtracting as much as possible the residual speckle noise. The LOCI algorithm is a very efficient way of combining a set of reference images to subtract the noise of a given image. Although high contrast performances have been achieved with ADI/SSDI/RSDI & LOCI, achieving high accuracy photometry and astrometry can be a challenge, due to various biases coming mainly from the inevitable partial point source self-subtraction for ADI/SSDI and how LOCI is designed to suppress the noise. We present here several biases that we hare uncovered while analyzing data on the HR8799 planetary system and how we have modified our analysis pipeline to calibrate or remove these effects so that high accuracy astrometry and photometry is achievable. In addition, several new upgrades are presented in a new archive-based (i.e. performing ADI, SSDI and RSDI with LOCI as a single PSF subtraction step) multi-instrument reduction and analysis pipeline called SOSIE.

Keywords: Image processing, exoplanets

1. INTRODUCTION

The ground- and space-based direct imaging searches for exoplanets around nearby stars are plagued by partial atmospheric turbulence adaptive optics corrections and/or imperfect optics that are generating time-varying speckles,[1] with some changing rapidly (from the atmosphere) while others more slowly (from the telescope and instruments). Those speckles are planet look-alikes that need to be removed to allow the detection of faint exoplanets.

One of the first few attempts to directly image exoplanets were performed using the reference star subtraction (what we could call Reference Star Differential Imaging or RSDI)[1] and a simple implementation of the SSDI[2] technique. These techniques were mainly limited by seeing evolutions, low optical drifts and non-common path aberrations that have limited the noise subtraction to less than a factor 10. With the invention of the Angular Differential Imaging (ADI) observing technique,[3–5] the effect of slowly evolving "quasi-static" speckles has been greatly reduced. The ADI technique uses the intrinsic field-of-view (FOV) rotation with time of altitude/azimuth telescopes to decouple the light from quasi-static speckles from that of the exoplanets. The instrument is setup to track the telescope pupil while the field is left to rotate with time. Since the optical path of the telescope and instrument is static with time, quasi-static speckles stay fixed on the image, though possibly slowly evolving in intensity or structure due to flexure as the telescope is tracking a target or other effects like temperature or pressure variations. During an observation, any planets located in the FOV are slowly appearing to revolve around the star (this rotation is due to the Earth rotation and not actual planetary motion, of course.) Filtering algorithms, like the original sequential differencing[3,5] or more advanced ones like LOCI[6] or ANDROMEDA,[7] can be used on a sequence of exposures to remove what is not rotating with time (speckles) and keep what is rotating (background stars/galaxies or stellar/substellar companions).

Further author information: (Send correspondence to Christian Marois)
Christian Marois: E-mail: christian.marois@nrc-cnrc.gc.ca, Telephone: 1 250 363 0023

Adaptive Optics Systems II, edited by Brent L. Ellerbroek, Michael Hart, Norbert Hubin, Peter L. Wizinowich,
Proc. of SPIE Vol. 7736, 77361J · © 2010 SPIE · CCC code: 0277-786X/10/$18 · doi: 10.1117/12.857225

The usual ADI speckle subtraction algorithm works as follow: for a given image sequence, the image subtraction algorithm selects a subset of images of the sequence to subtract the speckle pattern of a particular image if enough field-of-view (FOV) rotation ($\sim \lambda/D$) as occurs to avoid self-subtraction of point sources. The speckle subtraction efficiency is proportional to how much the images are correlated with time and how fast the FOV is rotating (function of the observation hour angle, object declination and telescope latitude). On-sky contrast gains of the order of 10-100 have been achieved with this technique[5,6] for hour-long sequences. In the near future, more advanced instruments, like the Gemini Planet Imager, will acquire images at many wavelengths without non-common path aberrations, allowing the Simultaneous Spectral Differential Imaging (SSDI)[8] speckle subtraction method, or the similar spectral deconvolution technique,[9] to be used to its full potential along with ADI, further improving the contrast by subtracting the atmospheric turbulence speckle noise.

The LOCI algorithm is a powerful algorithm to optimally combine a set of reference images to minimize the noise, after subtraction, of a given image of interest. The algorithm searches for a set of coefficients that minimize the residual image noise by finding those that satisfy the zero sum of the partial derivative of the residual subtracted image standard deviation with respect to the coefficients. The algorithm can be summarized as simply solving an $Ax = b$ problem, where A is a correlation matrix (a $n+1 \times n+1$ matrix for n reference images and one image of interest), x, the $n+1$ coefficient vector that we are searching, and b, the correlation vector of the image of interest with all the reference images (a $n+1$ vector). For ADI and SSDI, some LOCI coefficients are forced to zero to avoid significant point source self-subtraction. The algorithm is run in small image sections to perform the subtraction locally and to allow as much flexibility as possible to fit and subtract the image of interest. See Lafrenière et al. 2007 for more details about how LOCI is implemented.

The ADI, RSDI and SSDI observing techniques along with LOCI have been used to perform the initial surveys for planets orbiting nearby stars, but generally little attention has been given into insuring that the implemented speckle-filtering algorithm delivers a reliable photometry and astrometry when actually confirming a bound companion. The discovery of the HR8799 planetary system[10] (a star that transits 2 degrees from Zenith at Mauna Kea) has shown the limitations of a basic LOCI implementation for highly non-linear fast FOV rotation cases.

Determining the various LOCI biases is crucial. Scientific interpretation of planetary atmospheric and orbital properties, especially upcoming second generation large scale exoplanet imaging campaigns, may require one percent photometry and milliarcsecond (mas) astrometric accuracy. This paper summarizes the various LOCI biases that we have discovered, and the solutions that we have implemented, as well as upgrades that we have developed to further enhance the contrast. The overall modifications are now included in a multi-instrument (NIRI at Gemini North, NICI at Gemini South, NIRC2 at Keck2, NACO at VLT, NICMOS2 at HST and GPI) reduction package that we call SOSIE (so-ze), for Speckle-Optimize Subtraction for Imaging Exoplanets (the name means "twin or identical" in French). The SOSIE pipeline is the main reduction tool for the International Deep Planet Survey (IDPS), a ADI/SSDI/RSDI direct imaging exoplanet survey that is currently ongoing at several observatories.

2. THE SOSIE PIPELINE

The SOSIE pipeline was designed to answer the complex problem or reducing and analyzing similar high-contrast imaging data acquired with various telescope configurations (IDPS survey). The chosen architecture is actually quite simple and is illustrated in Fig. 1.

The initial software (step 1) reads the individual image headers to convert all necessary keywords (object name, integration time, coadds, hour angle, wavelength and observatory latitude) into a standard set of keywords. After combining flat field, dark and (if needed) sky images, reduction software (step 2) performs the initial reduction (dark subtraction, flat fielding, sky subtraction, bad pixel correction, distortion correction (if known) and image zero padding (image padding is necessary to avoid loosing the image corners when rotating back the images to align their North axis when using the ADI technique)). The third program (step 3) is then used for PSF centering. Due to various observing configurations (with/without coronagraph or unsaturated/saturated images), several options are left to the user – peak centroid (good for unsaturated data or when a coronagraph

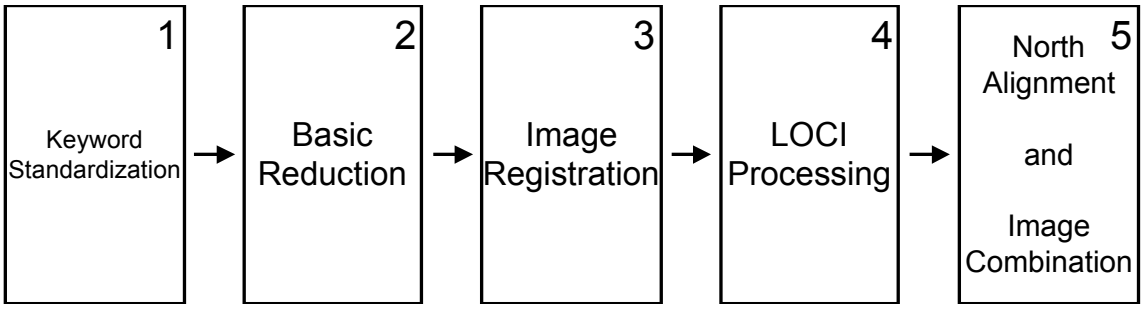

Figure 1. The SOSIE reduction pipeline.

is used and the PSF core is visible through the focal plane mask), cross-correlating inside a specific region (for saturated PSFs or when a coronagraph is used and the PSF core is not visible though the focal plane mask) or a cross-correlation in a section with a reference PSF (a PSF that has been previously register at the image center). If the PSF core is visible, a flux renormalization option is also available to correct for sky throughput and/or Strehl variations and to insure a constant PSF core flux inside a given aperture. The LOCI PSF subtraction (step 4) is then run in 2 different ways. A first quick reduction is performed in large ($50 \times 50\lambda$/D) square sections to quickly (few minutes for $1024 \times 1024 \times 100$ sequences) detect obvious candidates. A second slower LOCI reduction with smaller sections is then performed near the image center. An iterative Simulated Annealing (SA) LOCI parameter optimization (see Sec. 4.3) was implemented and can be run at several separations to find optimal LOCI parameters as a function of angular separation. Instead of minimizing the noise, this new optimization maximizes the point source signal-to-noise ratio. The point source residual signal is obtained using unsaturated data (artificial planets that are elongated in azimuth to account for the field rotation during an exposure) and the derived LOCI coefficients for each LOCI sections (so accounting for partial self-subtraction of the ADI and SSDI techniques). Once an optimal set of parameters have been found, the full reduction is performed for the image. Images are then rotated to align their North axis and median combined (step 5). The two LOCI reductions are finally combined into a final image. The simulated artificial point sources of each LOCI sections are also used to produce a template LOCI-subtracted PSF that can then be used to normalize the contrast curve or to fit a point source PSF (astrometry/photometry determination).

The architecture chosen to assemble reference images to subtract the noise of a given image is an evolution of what was presented in the original ADI/LOCI paper. Instead of restricting the LOCI algorithm to a single sequence of an object, all reduced images of all objects are stored in an archive, allowing the algorithm to have access to a vast array of reference images. In addition, if a multi-band/integral field spectrograph is used to acquire data, SSDI speckle suppression is performed in the same step as the ADI and RSDI techniques (see Fig. 2). The LOCI-based SSDI speckle suppression is still being implemented in SOSIE and it will be the subject of an upcoming paper (a basic version of the algorithm is currently being used for NICI dual-band data).

3. ASTROMETRY & PHOTOMETRY BIASES

There are many effects that can bias the point source photometry and astrometry when using the ADI/SSDI/RSDI observing techniques. Some are obvious, like sky throughput and/or Strehl variations for ground-based imaging, while others (see below) can be more complicated to properly calibrate.

3.1 Candidate Misalignment Bias

If images of a sequence are misaligned, the image combination step will lower the sensitivity to faint sources, the photometry of detected candidates will be underestimated and the astrometry may be offset. We have identified the following sources of misalignment:

1. Image-to-image registration error (if the PSF core is not visible). If the core is visible, then this effect is accounted for when calculating relative photometry/astrometry since the primary will be offset by the same

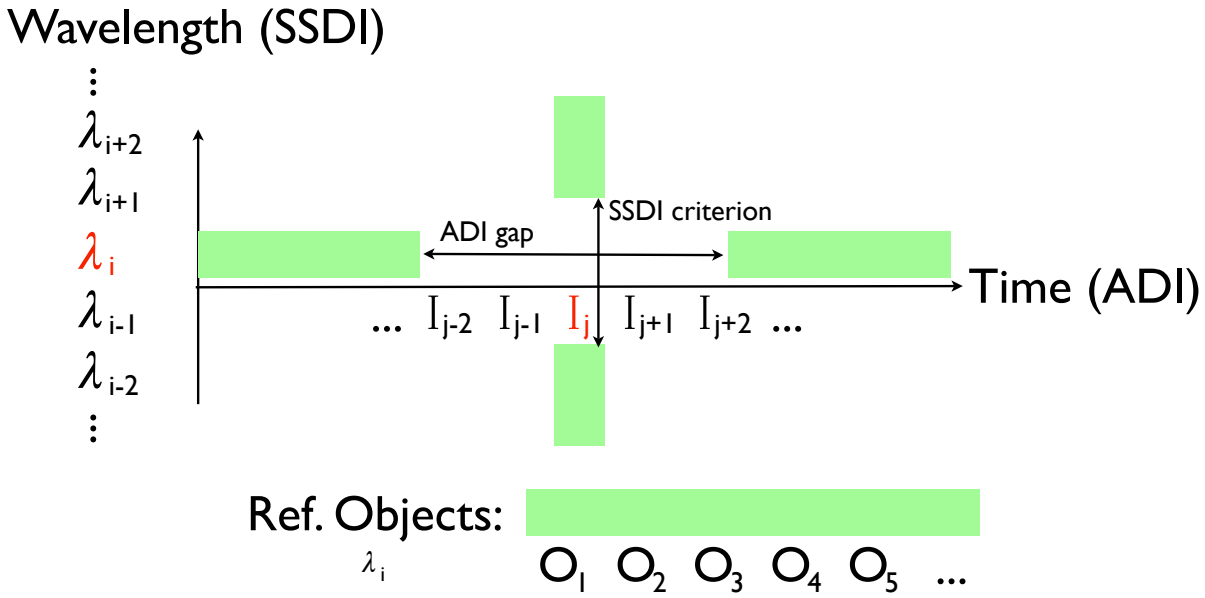

Figure 2. LOCI reference scheme. Reference images can be selected on the same object, but at a different time (ADI) using a minimal rotation gap to avoid self-subtraction. Reference images can also be selected in polychromatic image cubes (series of images acquired simultaneously, but at a different wavelength, i.e. for SSDI imaging). An SSDI criterion is selected to limit the point source self-subtraction that is a function of the flux differences between wavelengths and how much a point source has radially moved after the spatial magnification (to align speckles). Finally, the algorithm can also search into a reference star archive to find similar observations at the same wavelength (RSDI). All the good reference images (green areas) are then selected to run the LOCI algorithm.

amount). This is a fundamental effect and its impact needs to be estimated using a realistic registration error "guess".

2. PSF elongation: if significant FOV rotation occurs during an integration, point sources will be elongated along the azimuth axis. Since the elongation will change with time and separation relative to the primary, this effect needs to be evaluated using elongated artificial point sources.

3. Local optical distortions: As the FOV is rotating with time, point sources will be moving through various parts of the instrument optics, possibly being affected by local optical distortions. Instead of revolving around the star following the expected parallactic rotation rate curve, a companion may change separation, slow down or accelerate with time. The distortion needs to be estimated (or known to be negligible) or an unknown error is introduced in the photometry/astrometry analysis. This effects importance can be estimated if the point source is bright enough that it can be detected in single exposures and its position followed in time. Test images of known moderate-contrast binaries are another way to estimate this effect.

4. Overall image offset: if an entire sequence of images is offset relative to the true primary center (the field rotation axis), the point source's PSF will then follow a small circular motion when rotating the images to align their North axis. To try to minimize this error, we have implemented a "rotation axis finder" that is shifting the entire sequence of images (after LOCI processing) following a grid pattern and looking for the rotation axis position that maximizes a detected point source SNR.

5. North angle determination. Estimating accurately the North axis position of an ADI image can be very tricky, especially for a target that transits near the local Zenith. The exact offset of the time stored in

the header (start or end of an exposure) becomes critical, while other effects, like the tilt of the as-built telescope mount relative to the local vertical will also impact how the FOV will be rotating with time. If the parallactic rotation rate is changing significantly during the length of an exposure (near Zenith transits), the North axis needs to be shifted toward where the rotation rate is the slowest. Properly calibrating the ADI reduction/analysis software can be done by observing a binary system that transits near (5-10 degrees) from the local Zenith (using very short integrations to avoid PSF smearing) and by determining the observed parallactic angle rotation curve.

3.2 LOCI Optimization Section Finite Size

One of the key LOCI parameter when using the ADI observing technique is the rotation gap needed to select good reference images out of the observing sequence. The idea is to select images that have sufficient FOV rotation relative to the image that we want to subtract to avoid significant point source self-subtraction. For efficient reasons, the LOCI optimization sections can be large. Large sections can contains a large range of radial separations while the LOCI algorithm uses a single rotation gap for the entire section. The resulting effect (see Fig. 3) is that the inner part of the LOCI sections are analyzed with a smaller rotation gap (more self-subtraction), while the outer part of the section is reduced with a larger gap (less self-subtraction). At small separations and if the rotation gap is chosen to be less than a λ/D, significant throughput variations can occur. For full annulus sections, the LOCI throughput will be a saw tooth-like wave. It is interesting to note that if annulus sections are used, this effect will not average-out with FOV rotation since the candidate point source will always be located at the same radial separation.

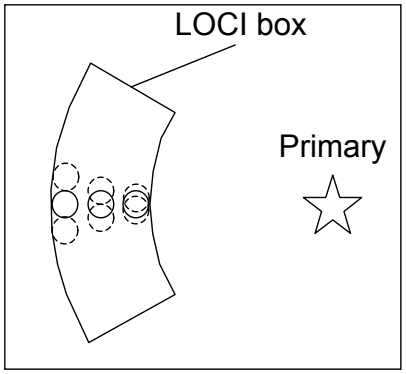

Figure 3. LOCI section point source variable throughput. For a motion gap that is selected at the middle of the LOCI section, all point sources located closer in will have more self-subtraction while point sources located near the outer edge will have less, resulting in a saw tooth-like throughput curve.

There are several ways to properly calibrate this effect. One obvious technique is to use artificial point sources that are located at the same radial separation as the candidate point source (if artificial point sources are always located at the middle of the LOCI sections, then this effect is never properly corrected). Another approach that we have implemented is to use a spiral distribution of LOCI sections. With a spiral distribution of sections, as the FOV is rotating, the position of the candidate point source is changing relative to the sections, thus averaging this effect. The reduction can be repeated by rotating the spiral distribution of sections around the PSF, thus further averaging the effect. If full annuluses are used, another solution that we have implemented is to use point sources that are added near the inner and outer parts of the annulus and a throughput function is derived to simply normalize the LOCI-process image and contrast curve.

3.3 Non-Symmetric Black Shadows

LOCI is mainly being used to analyze a set of images of a given object acquired in ADI and/or SSDI mode. This means that the candidate that we are trying to detect is also in the reference images. For ADI, a motion gap

needs to be selected to reject some images to avoid point source self-subtraction. Generally this motion gap is of the order of $\sim \lambda/D$. The reference PSF to subtract the speckle pattern of a given image is then constructed using a linear combination of all the reference images. Since the PSF speckle pattern is constantly evolving, images acquired with the least amount of time differences are usually the ones that are the most correlated with the image to subtract; they are thus the images that mostly contribute to the reference image. This means that the LOCI-derived reference image will have some planet flux near the candidate location, mostly at the motion gap criterion (thus $\sim \lambda/D$ away). The final process image will thus show the candidate with some leading/trailing dark shadows. The dark shadows will usually partially overlap the candidate point spread function, thus some light will be lost (photometry bias). In particular circumstances, it is possible for LOCI to produce a shadow that is darker on wide side of the candidate PSF than the other. This usually happens when observing objects that transits near Zenith while having an observing sequence that is offset relative to the object time of transit (as an example, imagine a sequence that start an hour before transits and finishes 10 minutes before transit). The FOV will be rotating slowly in the first 40 minutes of the sequence, but will significantly speed-up for the last 20 minutes. On average, the candidate in the reference images that are acquired at the start of the sequence are all piled-up over each other, generating a point source-like very dark shadow while images acquired near Zenith have move quite a lot, stretching the shadow. This shadow asymmetry is resulting in more flux being removed from one side of the candidate PSF than the other (astrometry bias, see Fig. 4).

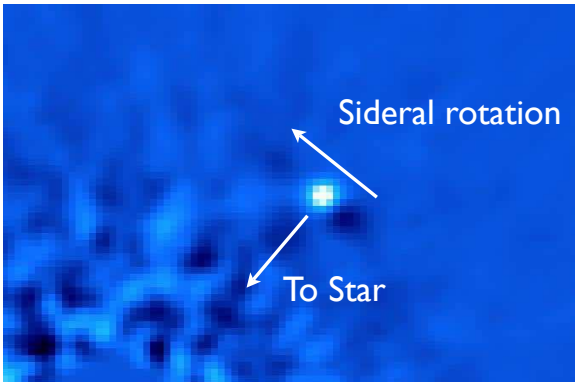

Figure 4. A Gemini North Altair/NIRI HR8799c asymmetric black shadow example.

Artificial companions can again be used to properly calibrate this effect. Using a larger motion gap to avoid overlapping the candidate between the images is also an option, although a larger motion gap usually means a lower SNR and less accurate astrometry/photometry.

3.4 Non-Uniform Sensitivity

The LOCI algorithm as originally presented uses a correlation matrix to determine the coefficients to multiply a set of reference images (usually acquired on the same object, but at a different time) to subtract the speckle noise of the original image.[6] In specific cases, a photometric bias can be introduced if large flux variations exist inside the image section where the LOCI algorithm is run. The regions that are the brightest will have more weight in the correlation matrix and the algorithm will work harder to remove the noise at those locations. This flux variation may come from a "patchy" PSF (HST) or radial intensity profile (ground-based data). This means that any point sources located in bright regions will have a lower throughput than point sources located in fainter areas. The noise following a LOCI reduction may thus look uniform, while the actual sensitivity to point sources may be strongly non-uniform, possibly leading to an overestimation of the contrast achieved by the reduction. Note that even if point sources are added to calibrate the contrast curve, depending where those sources are added, they may not be properly calibrating for this effect. This problem is simply due to the planet flux that is included in the LOCI correlation matrix. A technique that is sometime used to achieve better throughput is to reprocess the images while putting a NAN/zero mask over the candidate when calculating the correlation

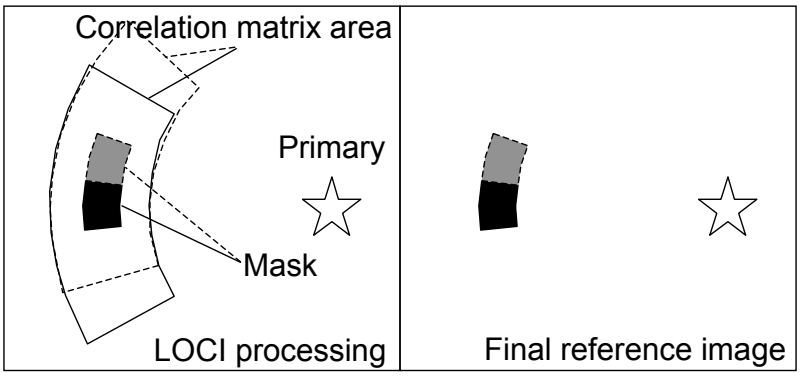

Figure 5. Generating the reference PSF with the LOCI local masking technique. The left panel shows how the correlation matrix is calculated for a certain annulus and angular separation (the calculation is shown for 2 azimuth positions represented by the solid and dashed lines). In the LOCI section, a small area is masked out of the correlation matrix calculation to derive the LOCI coefficients. The reference PSF section is then obtained for the area inside the mask and it is then copied into the final reference image (right panel).

LOCI matrix while keeping all other LOCI parameters the same. Such mask is insuring that the candidate flux throughput is improved (flux no longer part of the correlation matrix), but the final LOCI-process image may still be limited by a non-uniform sensitivity. The mask will increase the point source throughput, but the noise elsewhere at the same separation will be treated differently (that noise will be part of the correlation matrix, thus will have a lower throughput, while the noise located on the planet will have a higher throughput); such image cannot be used to derive an accurate photometry or astrometry errors.

To overcome the non-uniform sensitivity and planet-mask issues, a $\sim \lambda/D \times \lambda/D$ mask is added to remove part of the image section used to calculate the LOCI correlation matrix (see Fig 5). The reference image section is then assembled without that mask and only pixels inside the mask are copied into the final reference image. The mask and LOCI section are then moved around at all possible locations to reconstruct the entire reference image. With this approach, both the noise and planets have been masked the same way, thus such image can be used to accurately derive a point source photometry and astrometry errors.

This effect was first discovered when trying to use the LOCI algorithm to find HR8799c and d in the HST 1998 NICMOS 2 data (PI E. Becklin). If the LOCI algorithm is run in an annulus, HR8799c is clearly visible (see Fig. 6 and Marois et al., in preparation). If additional 10σ sources are added at the same separation of HR8799c but at different azimuth angles, at some locations the additional point sources are nearly invisible.

4. SOSIE UPGRADES

Various photometry/astrometry issues were discussed in the previous section. We now turn our focus to several upgrades that were implemented since the original publication of the ADI technique[5] and LOCI algorithm.[6] Most of these upgrades were developed very recently, following the HR8799 planetary system discovery.

4.1 PSF Fitting After LOCI Processing

Deriving accurate photometry and astrometry with LOCI can be difficult, especially with the many biases presented in Sec. 3. A simple aperture photometry and PSF core Gaussian fitting is usually not satisfactory; the use of artificial sources is inevitable. To avoid having to do several reductions with/without artificial sources, the SOSIE pipeline generates template PSFs in each LOCI optimization sections while processing the images, using the same LOCI coefficients derived to subtract the section. This template PSF can then be used to subtract any candidate and derive its flux and position to high accuracy. Once the planet position and flux are known, an additional reduction can be run while subtracting the planet flux in all images to check the goodness of the fit. Another reduction can also be run by removing the planet flux in all reference images, resulting in a

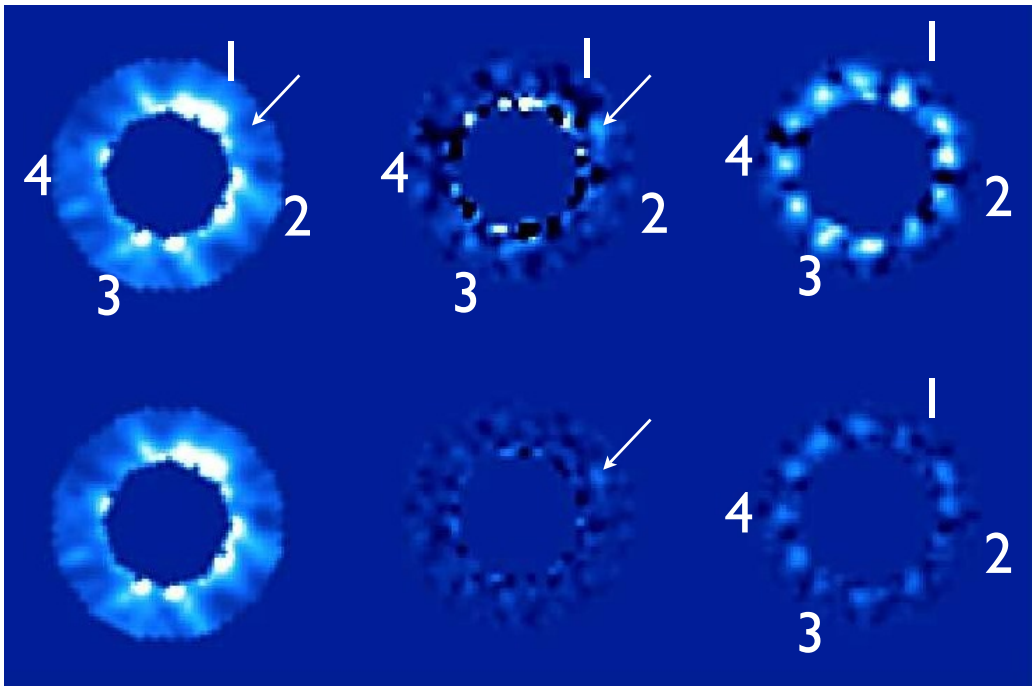

Figure 6. HST NICMOS 2 HR8799 data with (upper row) and without (bottom row) the local masking technique. The first column to the left shows the register HST PSF inside the annulus of interest while the middle column shows the LOCI process images. The right most column shows the LOCI process images, but with added artificial 10σ point sources (added every 30 degrees in 12 independent reductions). Note the uniform noise in the bottom middle panel while the same reduction (bottom right panel) shows strong artificial point sources intensity fluctuations. The above middle panel shows a non-uniform noise but better point source throughput (and an intensity fluctuation that is correlated with the noise). In particular, look at the positions 1 to 4 (areas where an artificial source fall on a bright area), where the noise is higher in the above panels, the throughput is less in the bottom panels. The white arrows point toward HR8799c position. Note the planet position in the HST register image (upper left panel), it falls right on a dark area for that HST roll angle, explaining why it is easily visible in the non-mask reduction (bottom middle panel). The upper middle panel shows that HR8799c SNR is not as good as one would have thought from a non-mask LOCI analysis.

nice dark-shadow-free image to be obtained since most of the candidate self-subtraction have been removed (see Fig. 7).

4.2 SSDI with SOSIE

A very basic SSDI algorithm is currently implemented in SOSIE for analyzing NICI dual-band data. The pipeline simply does the LOCI reduction with/without the simultaneous image in the reference pool of images, similar to what was presented by the NICI campaign team.[11] A more advanced code is currently being implemented to better use the multi-wavelength simultaneous images that we will get with the Gemini Planet Imager (GPI[12]). Several expected template spectrum (e.g. with deep spectral features, or a flat spectrum similar to the star etc.) will be given to SOSIE to judge what ADI, RSDI or SSDI images can the code use to find an optimal SNR at a given wavelength and separation. Once a candidate has been found, the LOCI reduction is then iterated at that separation while updating the input spectrum to converge to the candidate spectrum that maximizes the candidate SNR. While the ADI reference image criterion is defined has a certain amount of FOV rotation, the SSDI criterion is instead defined as a certain amount of flux subtraction in a $\sim \lambda/D$ aperture. This criterion is selected mainly because for SSDI, the planets are moving along the radial axis with wavelength due to the spatial chromatic magnification that was applied to align the speckles (PSF chromaticity) and the candidate flux variation between wavelengths.

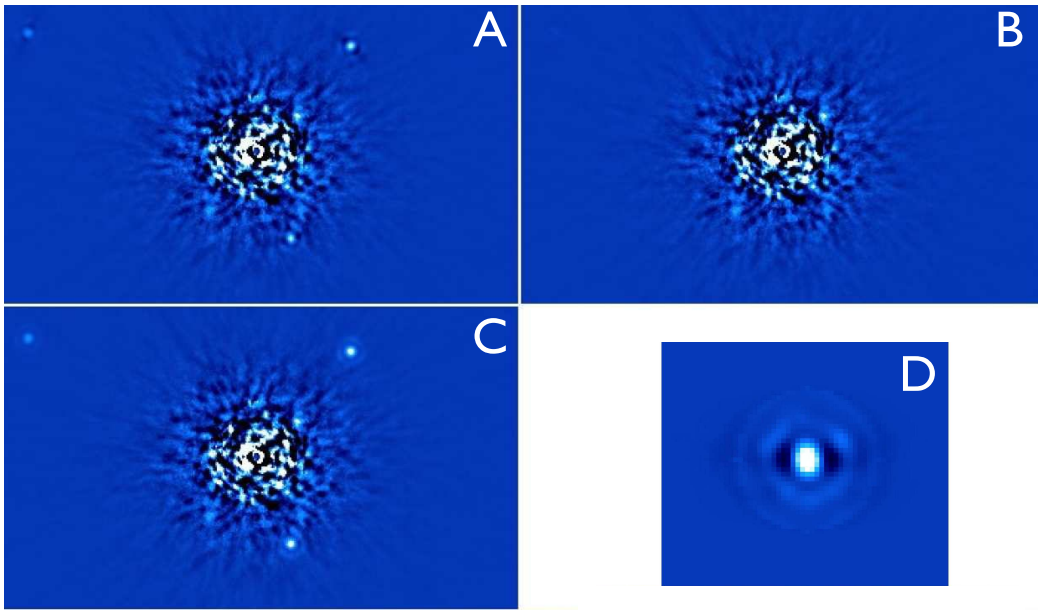

Figure 7. LOCI template PSF fitting. The panel A shows an HR8799 K-band standard LOCI reduction. The B panel shows the same reduction after subtracting the three planets in all images of the sequence. The C panel shows the reduction after subtracting the three planets in all reference images (note the removal of all dark shadows). The D panel shows one of the LOCI template PSFs (before rotation) used to derive the photometry and astrometry of one the three planets.

For an example how the algorithm works, consider a methanated planet showing a strong 1.6μm absorption bandhead. When trying to subtract the PSF bluer of 1.6μm (where the planet is bright), the LOCI algorithm will be able to choose images that are just a bit redder, where the planet PSF still overlap but where the planet is much fainter, resulting in very little planet flux being removed. When analyzing a wavelength inside the methane absorption bandhead, the algorithm will select wavelengths that are much bluer/redder to avoid overlapping the planet PSF and suffer significant self-subtraction, especially from wavelengths where the planets is much brighter.

4.3 LOCI Parameter Optimization with Simulated Annealing

Since the LOCI analysis is local, a specific area where the analysis is performed need to be defined. In addition, when using ADI and SSDI, a rotation gap or a flux subtraction criterion need to be selected. If many images are part of the reference pool of images, the number of acceptable images needs to be limited (see below); finding an optimal set of parameters is thus not trivial. In addition, the LOCI algorithm was developed to minimize the noise, while in practice, we would like to maximize the point source SNR. For these reasons, we have developed an optimization scheme based on Simulated Annealing (SA) to search for an optimal set of parameters that maximizes the point source SNR in each LOCI optimization sections. Since the optimization can become very CPU intensive, it is only performed at a few key separations before performing the full LOCI analysis in the entire image. The iterative algorithm is summarized below:

1. An initial set of parameters is first chosen
2. The LOCI analysis is performed in the LOCI section
3. The artificial point source SNR is calculated
4. Parameters are randomly changed inside an allowable range and the reduction is repeated
5. Updated set of parameters are kept for the next iteration given a probability function (100% if better SNR, $<$ 100% if SNR is lower).

6. The probability function to retain lower SNR configurations is reduced at each iteration step.

It was found that the ADI rotation gap and overall LOCI section size have only a marginal impact of the final SNR (SSDI optimization has not yet be fully tested). One key parameter is the number of reference images that are used to subtract the PSF. This problem was traced back to the LOCI matrix inversion that is prone to numerical noise that can prevent the algorithm to converge to an optimal solution. The LOCI algorithm is based on the sum of the partial derivatives of the image standard deviation with respect to the coefficients that is equal to zero. If the coefficient function has many secondary minima, many coefficients combinations can solve this system of equations. The inversion usually becomes unstable if the reference images are uncorrelated with the image to subtract (read/sky noise limited or rapidly evolving PSF; the algorithm is then trying to fit noise) or when the number of reference images is of the same order as or greater than the number of pixels in the LOCI optimization section (too many free parameters, the algorithm is then starting to fit the image pixel-per-pixel, possibly resulting in a very low noise subtracted image, but where any point source throughput is greatly reduced). If the masking scheme presented in Sec. 3.4 is used, some pixels are removed from the fit. If the fit becomes ideal (pixel-to-pixel fit), pixels inside that mask will become noisier to allow for a better fit elsewhere. Since only the pixels inside that mask are retained in the final reduced image, the masking technique approach can be used to evaluate the severity of this effect. This problem was first identified with the HST 1998 HR8799 data where more than 200 images (acquired on different objects but at the same wavelength) are used as reference images to subtract the HR8799 PSF (the usual ADI-only sequences obtained on ground telescope are usually not prone to this problem due to the limited number of images, but such problem may be encountered when using a large archive of reference images). In the image inner part where HR8799d is located, the noise when performing a full matrix inversion (IDL *invert* routine) is significant (see Fig. 8).

After optimizing the number of allowable reference images to use, it was found that such limitation can significantly decrease the noise in the final LOCI reduction in certain regions (a factor of 10 for our case), thus improving the matrix inversion accuracy to converge to the best solution (absolute minimum) with the available reference images (see Fig. 8). The subset of images to use during the LOCI processing are not selected at random. A global cross-correlation algorithm is first used to sort-out the references that are the most correlated with the image that we want to subtract to the least. The SA optimization algorithm thus always use the most correlated images and gradually add or remove less correlated images for LOCI processing.

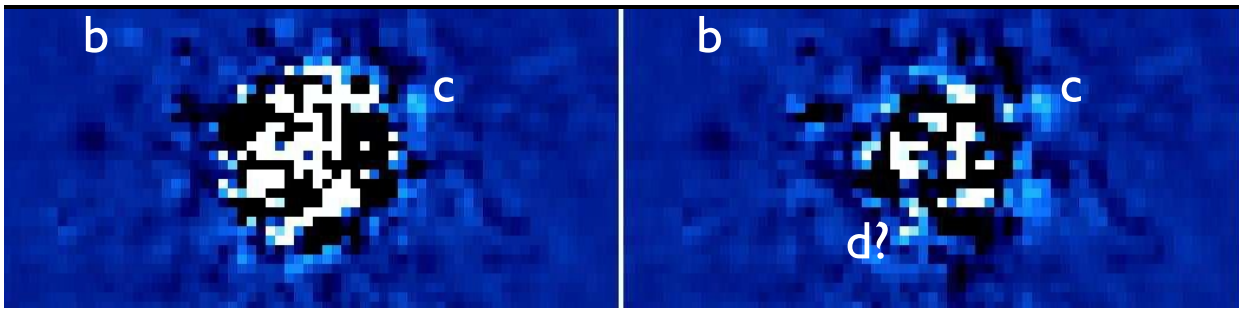

Figure 8. Left panel shows the HST HR8799 data using all reference images (215), while right panel shows the same reduction, but after limiting the number of reference images to use at each angular separation. At wide separations, all images are used, while at small separations, the algorithm found out that $\sim$ 80 images is the optimal solution. The noise at small separations has been lowered by a factor 10. HR8799c and possibly d have been detected (see Marois et al., in preparation for more details).

Note that we also tried a Singular Value Decomposition (SVD) matrix inversion approach with a singular value cutoff to limit the number of reference images, but performance was somewhat inferior to the algorithm mentioned above. The SVD method did manage to improve compared to the full inversion using all references, but it converges, for the HST data reduction case, to a noise level that is 30-50% higher than the cross-correlation-selected solution. One of the main advantages of the SVD matrix inversion technique is that the reference

restriction is performed "on the fly" without having to rely on an iterative optimization; it is thus much easier to implement and less CPU intensive.

4.4 L- and M-bands LOCI-based Sky Subtraction

After the HR8799 discovery, it was important to acquire as many photometric points on all three planets to help characterize their atmosphere. The longer wavelengths, L- and M-bands, can be use to better estimate a planet overall luminosity (and better mass estimates when compared to cooling tracks) as well as study the importance of non-equilibrium chemistry.[13] For ground-based observations, one of the main challenges at those wavelengths is the background subtraction. At the Keck telescope, the background subtraction is further complicated by the image derotator, located near the input focus of the AO bench, that is producing a time-evolving spatially-non-uniform thermal background. The time-evolution is generated by the instrument rotation and also the deformable mirror, which modulates the thermal background as it is reimaged onto the detector in a seeing-dependent way. The standard technique to subtract the thermal background is to take images of the science image using a dither pattern that are median to generate a sky image and/or acquire sky images. To improve the master sky frame correlation with the thermal background to subtract, we have implemented a LOCI-based background subtraction routine in SOSIE. The sky subtraction algorithm works as follow: just after making the basic image reductions, the star position is estimated. The algorithm then searches through the sequence of images for ones where the star is located at another widely separated position on the detector (dither sequence) or for sky images (no star on the detector). The LOCI algorithm is then used to combine those sky images into an optimal background image. On a Keck M-band sequence where an unsharp mask was used to remove the low-spatial frequencies, a subtraction gain of a factor 2 for the $\sim \lambda/D$ spatial frequencies was obtained relative to the standard sky images median combination (see Fig. 9), resulting in a factor 4 gain in integration time where the images are background noise limited.

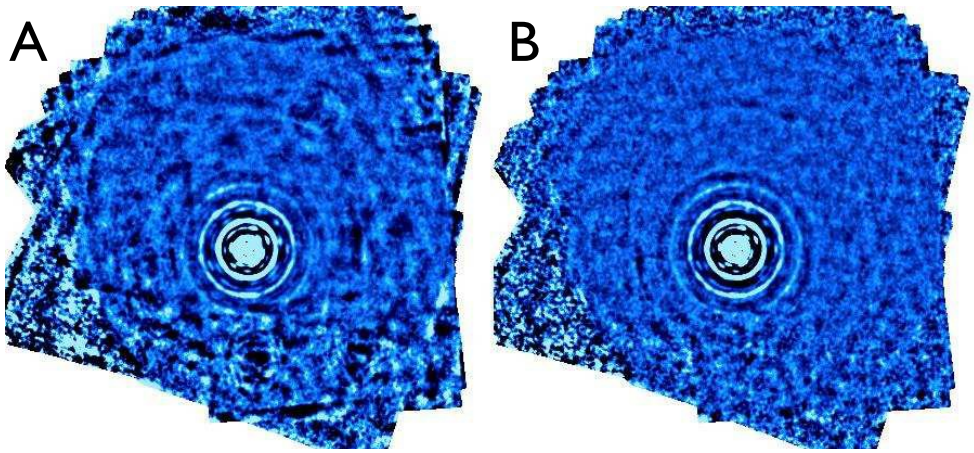

Figure 9. SOSIE Lp- and M-band new LOCI-based sky subtraction scheme. The A panel shows the M-band sky subtraction using a standard technique (median of sky images) while the B panel shows the same image, but after subtracting a sky image that is assembled using LOCI.

5. CONCLUSIONS

The SOSIE pipeline is being developed in a way that it will allow a full archive-based (ADI/SSDI/RSDI in a single step) polychromatic PSF subtraction scheme based on LOCI. All images that are being reduced and registered will be stored in an archive that can be access for PSF subtraction if similar images (of this object or others) are made with the same configuration in the future. This is envisioned to be crucial to discover planets or disks at very small angular separations (where ADI and SSDI imaging can be limited) with next generation instruments like GPI. The pipeline is also configurable to solely do LOCI for ADI and RSDI, while not performing SSDI to test other algorithms, like spectral deconvolution. Since both LOCI and spectral deconvolution are linear operators,

it will be interesting to see if one is better than the other. If many polychromatic images are available, LOCI is equivalent of doing a high-order fit on an area, while spectral deconvolution is fitting a low order polynomial pixel-per-pixel.

Many modifications and upgrades of the ADI/SSDI LOCI processing technique were presented in this paper with several more to come. The complex problem of obtaining accurate photometry and astrometry with the various LOCI biases was discussed. The many SOSIE optimization steps that were presented are CPU intensive. Careful pipeline optimization and migrating to a multi-CPU super-computer architecture will be required in the near future.

ACKNOWLEDGMENTS

Thank you to David Lafrenière, Mickael P. Fitzgerald, Dimitri Mawet and Laurent Pueyo for discussions. Portions of this work performed under the auspices of the U.S. Department of Energy by Lawrence Livermore National Laboratory under Contract DE-AC52-07NA27344.

REFERENCES

[1] Marois, C., Doyon, R., Nadeau, D., Racine, R., and Walker, G. A. H., "Effects of quasi-static aberrations in faint companion searches," in [*Astronomy with High Contrast Imaging*], Aime, C. and Soummer, R., eds., *EAS Publications Series* **8**, 233–243 (2003).

[2] Marois, C., Doyon, R., Nadeau, D., Racine, R., Riopel, M., Vallée, P., and Lafrenière, D., "Trident: An infrared differential imaging camera optimized for the detection of methanated substellar companions," *PASP* **117**, 745 (2005).

[3] Marois, C., [*La recherche de naines brunes et d'exoplanètes: Développement d'une technique d'imagerie multibande*], Université de Montréal, Montréal (2004).

[4] Liu, M. C., "Substructure in the circumstellar disk around the young star au microscopii," *Science* **305**, 1442 (2004).

[5] Marois, C., Lafrenière, D., Doyon, R., Macintosh, B., and Nadeau, D., "Angular differential imaging: A powerful high-contrast imaging technique," *ApJ* **641**, 70152 (2006).

[6] Lafrenière, D., Marois, C., Doyon, R., Nadeau, D., and Artigau, E., "A new algorithm for point-spread function subtraction in high-contrast imaging: A demonstration with angular differential imaging," *ApJ* **660**, 770–780 (2007).

[7] Mugnier, L. M., Cornia, A., Sauvage, J.-F., Védrenne, N., Fusco, T., and Rousset, G., "Maximum likelihood-based method for angular differential imaging," in [*Adaptive Optics Systems*], Hubin, N., Max, C. E., and Wizinowich, P. L., eds., *Proc. SPIE* **7015**, 233–243 (2008).

[8] Marois, C., Doyon, R., Racine, R., and Nadeau, D., "Efficient speckle noise attenuation in faint companion imaging," *PASP* **112**, 91–96 (2000).

[9] Sparks, W. B. and Ford, H. C., "Imaging spectroscopy for extrasolar planet detection," *ApJ* **578**, 543–564 (2002).

[10] Marois, C., Macintosh, B., Barman, T., Zuckerman, B., Song, I., Patience, J., Lafrenière, D., and Doyon, R., "Direct imaging of multiple planets orbiting the star hr 8799," *Science* **322**, 1348–1352 (2008).

[11] Artigau, E., Biller, B. A., Wahhaj, Z., Hartung, M., Hayward, T. L., Close, L. M., Chun, M. R., Liu, M. C., Trancho, G., Rigaut, F., Toomey, D. W., and Ftaclas, C., "Nici: combining coronagraphy, adi, and sdi," in [*Ground-based and Airborne Instrumentation for Astronomy II*], McLean, I. S. and Casali, M. M., eds., *Proc. SPIE* **7014**, 70141 (2008).

[12] Macintosh, B. and et al., "The gemini planet imager: from science to design to construction," in [*Adaptive Optics Systems*], Hubin, N., Max, C. E., and Wizinowich, P. L., eds., *Proc. SPIE* **7015**, 701518 (2008).

[13] Hinz, P. M., Rodigas, T. J., Kenworthy, M. A., Sivanandam, S., Heinze, A. N., Mamajek, E. E., and Meyer, M. R., "Thermal infrared mmtao observations of the hr 8799 planetary system," *ApJ* **716**, 417–426 (2010).